Characterizing Excavation Damaged Zone and Stability of Pressurized Lined Rock Caverns for Underground Compressed Air Energy Storage

Hyung-Mok Kim[1,4], Jonny Rutqvist[2], Ju-Hwan Jeong[3],
Byung-Hee Choi[4], Dong-Woo Ryu[4], Won-Kyong Song[4]

[1] *Energy and Mineral Resources Engineering, Sejong University, Seoul, 143-747 Korea*

[2] *Lawrence Berkeley National Laboratory (LBNL), Berkeley, CA 94720 U.S.A.*

[3] *South Mine Security Office, Ministry of Knowledge Economy, Hwasun, 519-805 Korea*

[4] *Korea Institute of Geoscience and Mineral Resources (KIGAM), Daejeon, 305-350 Korea*

Abstract

In this paper, we investigate the influence of the excavation damaged zone (EDZ) on the geomechanical performance of compressed air energy storage (CAES) in lined rock caverns. We conducted a detailed characterization of the EDZ in rock caverns that have been excavated for a Korean pilot test program on CAES in (concrete) lined rock caverns at shallow depth. The EDZ was characterized by measurements of P- and S-wave velocities and permeability across the EDZ and into undisturbed host rock. Moreover, we constructed an *in situ* concrete-lining model and conducted permeability measurements in boreholes penetrating the concrete, through the EDZ and into the undisturbed host rock. Using the site-specific conditions and, the results of the EDZ characterization, we carried out a model simulation to investigate the influence of the EDZ on the CAES performance, in particular related to geomechanical responses and stability. We used a modeling approach including coupled thermodynamic multiphase flow and geomechanics, which was proven useful in previous generic CAES studies. Our modeling results showed that the potential for inducing tensile fractures and air leakage through the concrete lining could be substantially reduced if the EDZ around the cavern could be minimized. Moreover, the results showed that the most favorable design for reducing the potential for tensile failure in the lining would be a relatively compliant concrete lining with a tight inner seal, and a relatively stiff (uncompliant) host rock with a minimized EDZ. Because EDZ compliance depends on its compressibility (or modulus) and thickness, care should be taken during drill and blast operations to minimize the damage to the cavern walls.

Keywords: Excavation disturbed zone (EDZ); Compliance; Lined rock cavern (LRC); Compressed air energy storage (CAES); TOUGH-FLAC simulator

1. Introduction

Along with pumped hydroelectric storage, underground compressed-air energy storage (CAES) is considered one of the most promising large-scale electric-energy-storage technologies. CAES is an approach by which excess electricity is used to compress air that is then injected into subsurface caverns (solution-mined cavities in salt deposits, or mines) or porous reservoirs (aquifers or depleted hydrocarbon reservoirs) (Succar and Williams, 2008).

A few underground CAES plants exist, including commercial plants in Huntorf, Germany, and McIntosh, Alabama, USA, as well as a pilot plant in Hokkaido, Japan, all constructed at a depth of 400 – 600 m. The two commercial CAES facilities were constructed in rock salt formations that can be found only in a few regions, not always near an energy source or demand. Moreover, the storage caverns at these facilities were located relatively deep below the ground surface to achieve sufficient ambient fluid pressure, thereby preventing air leakage and assuring mechanical stability.

Figure 1 demonstrates the conceptual model for CAES in underground lined rock caverns. Excess or off-peak power from wind and/or solar power is used to compress air and inject the compressed air to store in the cavern with an air tight concrete lining system. When power demand exceeds supply, the stored air is used to run a gas turbine generator and to provide the power to a grid. Because gas turbines typically expend approximately two-thirds of their power for compressing air, compressed air from a CAES fed into the gas turbine can substitute for one-quarter to one-half of the natural gas needed for a given amount of electricity generated. The CAES in underground lined rock caverns can be located at shallow depths, at significantly reduced construction costs, along with greater flexibility in site selection. If the lining is perfectly air-tight, the cavern pressure is transferred through the lining and sustained by a surrounding rock mass. Recently, Kim et al. (2012), showed that CAES in shallow lined rock caverns is feasible from a leakage and energy-efficiency viewpoint, provided that mechanical stability can be achieved.

Moreover, Rutqvist et al. (2012), studying coupled geomechanical and thermodynamic processes in underground CAES caverns for a similar kind of system, found that tensile stresses would develop in the concrete lining, but such stresses could be reduced when using an air tight inner seal (such as a rubber or steel liner) that would not allow pressurized air in the cavern to penetrate into the lining.

Construction of underground excavations in geological formations usually results in an excavation disturbed zone (EDZ), where significant changes in geomechanical, hydrogeological, and thermal properties may occur as a result of *in situ* stress redistribution and damage from the excavation process. The development of an EDZ depends on many parameters such as excavation method, tunnel geometry, rock properties, and *in situ* stress conditions. Many researchers have investigated the size and characteristics of EDZ through *in situ* tests, mainly at underground research laboratories (URLs), for studies related to radioactive waste disposal (Bäckblom and Martin, 1999; Sato et al., 2000; Hudson et al., 2001; Bossart et al., 2002; Kwon and Cho, 2008). The EDZ is relevant for radioactive waste disposal, since excavation damage creates an increase in permeability potentially several orders of magnitude higher than that of the undamaged host rock (Blümling et al., 2007). Consequently, an EDZ with raised permeability could affect the performance and safety of the repository, providing a preferential pathway for radionuclides to migrate. Barton (2007), reviewing a number of seismic measurements from numerous fields, showed that seismic velocity monitoring is useful in identifying and visualizing the disturbance around excavated caverns. In addition, numerical models (Golshani et al., 2007; Wang et al., 2009) have been developed for predicting the creation of EDZ under various geological conditions, by simulating the microcracking behavior of brittle rocks.

EDZ may also influence the performance of CAES and natural gas storage in lined rock caverns, particularly with respect to geomechanical stability and air-leakage potential. In this paper, we investigate the influence of EDZ on the geomechanical performance of CAES in shallow, lined rock

caverns, using newly acquired field data on EDZ properties around excavations which will be used for pilot tests on underground CAES in lined rock caverns in Korea. We first introduce engineering and hydrogeological characterization results for the EDZ around two lined rock caverns that have been constructed at shallow depth for CAES pilot testing. The EDZ was characterized by a seismic exploration method involving measurements of P- and S-wave velocities and permeability in boreholes. Incorporating the characterization results, we performed a numerical modeling study of coupled thermodynamic and geomechanical processes to investigate the effect of the EDZ on the geomechanical stability of the CAES caverns. We conclude with recommendations emphasizing the importance of minimizing the EDZ for optimum stability of CAES systems involving lined caverns at shallow depth.

2. A Pilot Test Program for CAES in Lined Rock Caverns at Shallow Depth

A pilot test program for underground CAES in lined rock caverns is being carried out in South Korea (KIGAM, 2010). This pilot test program is focused on the concept of underground, lined rock storage caverns at shallow depth, a CAES option that takes advantage of an engineered lining for air-tightness and stability. The concept provides flexibility in site selection and the potential construction-cost savings related to excavations at a shallower depth. The pilot test program aims at investigating the feasibility of the concept and to study the design of system components, including cavern, concrete plug, and lining materials.

Figure 2 presents a plane view of the pilot plant, including two storage caverns. These storage caverns are located in limestone at 100 m depth. They were built with a concrete lining and an inner seal, but the material of the inner seal differs in each. In one cavern, the inner seal is made of a butyl rubber sheets; in the other steel plates. In the lined-rock-cavern concept, the internal liners serve only to provide air tightness, with all the pressure applied to the lining surface (caused by highly pressurized air storage) transferred through the lining and sustained by a surrounding rock mass.

The caverns were excavated using drill-and-blast, but smooth blasting technique using lightly charged but closely spaced boreholes was employed at the perimeter of the caverns to minimize blast-induced damage and to obtain a smoother excavated rock surface. A smoother rock surface is beneficial to reduce the potential for tensile cracking of concrete linings, because the inner air pressure may induce a more uniformly distributed deformation and stress when transferred to the surrounding rock across a uniform concrete/rock interface. After excavation rock support was installed, including rock bolts and shotcrete (according to the usual practice in a tunnel construction). With an eye toward safety and potential local failure resulting from stress concentration and redistribution, the inner storage cavern was designed to be circular with a 5 m diameter. The thickness of the concrete lining differed in the two pilot test caverns: the one with an inner rubber sheet had a lining thickness of 500 mm, whereas the one with an inner steel plate had a lining thickness of 300 mm.

3. Characterization of Excavation Disturbed Zone (EDZ)

The EDZ at the pilot test caverns was characterized in terms of thickness, modulus, and hydrological properties, as described in the following subsections.

3.1 EDZ thickness around the cavern by a seismic exploration

A seismic exploration of P- and S-wave travel times (and velocities) was carried out to estimate the thickness of the EDZ around excavated caverns. The seismic exploration system (Figure 3) consisted of a triaxial geophone sensor (GS-14-L19, 28Hz), a trigger, and a data acquisition system (Geode, 24 channels).

Test boreholes—76 mm in diameter and 10 m long—were drilled perpendicular to the side wall of the caverns. A packer mounted with a triaxial geophone sensor was inserted into the boreholes and inflated for tight contact with the borehole wall (Figure 3b). Seismic waves were generated by striking the plate that was fixed on the cavern wall, using a trigger system (Figure 3c). S-waves

were generated by striking the plate in opposite directions, and their phase inversions were monitored by the geophone system.

Jeong (2010) has reported that the EDZ can be more effectively investigated by plotting the measured travel times as a function of distance from the cavern wall rather than wave velocity. In Figure 4, the slopes of curves for travel time change distinctly at approximately 0.6 m from the cavern wall, indicating a boundary between unaffected host rock and loosened EDZ rock adjacent to the tunnel wall. Table 1 shows the calculated average seismic velocities obtained from the reciprocals of the travel time curve slopes. At this specific test site, the average velocity in the EDZ was as low as 25% of that in the undisturbed host rock.

3.2 Hydraulic Characterization of Concrete Lining and EDZ

In situ borehole hydraulic tests were carried out to investigate the hydraulic properties of the concrete lining and EDZ around the underground excavated caverns. We constructed a concrete lining model at the pilot plant site (KIGAM, 2011) as shown in Figure 5 and drilled two different directional boreholes dedicated to *in situ* full-scale permeability tests. The dimension of the concrete lining model was 2400 mm x 1200 mm x 900 mm (length x height x width), with construction method and installation conditions identical to those for the CAES pilot plant caverns. As such obtained permeabilities would be adequate as input for analyzing the air-tightness performance of the CAES pilot plant. A longitudinal directional borehole (BH#1), 1.7 m in length, was used in testing and comparing the permeabilities of concrete lining matrix and construction joints. A transverse directional borehole (BH#2) with a length of 5 m, extending into the surrounding rock mass, was used for testing rock-mass permeabilities around the excavated storage cavern. Here, only the results of the transverse directional borehole are presented and used in the following analysis.

For permeability measurements, we employed a newly developed multi-packer hydraulic testing system designed for 76 mm diameter boreholes and short packer intervals of 200 mm (Figure 6). Using short test intervals, we could produce a permeability profile along the distance from the cavern wall and identify increments of permeability around the cavern. Multiple flow meters ranging from 50 g/hr to 20.2 kg/hr enabled us to perform a wide range of pneumatic and/or hydraulic tests at high precision, including pulse tests, constant flow, and pressure tests.

The estimated permeabilities for the concrete lining and surrounding rock mass are shown in Figure 7 as a function of the distance from the cavern wall. The figure shows that permeabilities for the 90 cm thick concrete lining range between 10^{-20} and 10^{-19} m^2. Note also that the permeability significantly increases to over 10^{-16} m^2 at the interface between concrete lining and rock mass. This relatively high permeability is attributed to imperfect bonding of the *in situ* installation, identified from borehole-wall image inspection. The permeabilities of the surrounding rock mass range from 10^{-20} to 10^{-18} m^2, and comparatively greater permeabilities of 10^{-17} to 10^{-16} m^2 could be found within the 1.5 m distance from the inner surface of the concrete lining (i.e., 60 cm from the excavated rock wall).

4. Numerical Evaluation of EDZ influence on Geomechanical Stability

We investigated the influence of the EDZ on the geomechanical performance of the CAES lined caverns, using numerical modeling. For this modeling effort, we used TOUGH-FLAC coupled analysis (Rutqvist, 2011), following a modeling approach and setup recently used by Kim et al. (2012) and Rutqvist et al. (2012) on an equivalent CAES system. The principles of TOUGH-FLAC coupled analysis are shown in Figure 8. A TOUGH2 (Pruess et al., 1999) to FLAC3D (Itasca, 2009) link takes multiphase pressures, saturation, and temperature from the TOUGH2 simulation and provides updated temperature and pore pressure to FLAC3D. After data transfer, FLAC3D internally calculates thermal expansion and effective stress using a maximum pressure taken from

the calculated pressures of the various phases—for example, air and water in this CAES simulation. Herein, we are using site specific-data and conditions from the pilot test site, focusing our analysis on the influence of the EDZ, incorporating EDZ properties characterized and summarized in the previous section.

4.1 Analysis Conditions

Model geometry and grid were similar to that used in Kim et al. (2012) and Rutqvist et al., (2012), except for EDZ thickness and properties, which have since been updated based on investigation at the pilot test cavern (Figure 9). It is a 2D model domain, corresponding to a 1 m thick vertical cross-section through the storage cavern, with a radius of 2.5 m, and with thicknesses for the concrete lining and EDZ of 0.5 and 0.6 m, respectively. The thickness of EDZ can be different from roof, wall and floor of excavated caverns but, it was considered to be uniform in our analysis in which overall geomechanical performance of pressurized cavern rather than localized failure was of interest. Initial conditions correspond to the conditions at the pilot tests located at a depth of 100 m in carbonate rock. This includes initial temperature of the rock mass around the cavern, which was 14°C, whereas the ground surface temperature was set to 11°C. Because they are within a mine still under operation, the pilot test caverns are located in unsaturated rock with the groundwater table far below. Vertical stress was set to be equivalent to the weight of overburden rock, calculated by the depth (100m) x density (2.75 g/cm^3); horizontal stress was set using the *in situ* stress ratio of 0.86 observed from the hydraulic fracturing tests at the depth of the pilot test site. The direction of maximum horizontal stress was sub-parallel to the cavern axis direction. Initial saturation of concrete lining was also required in the analysis, and was set as 0.85 (Abbas et al., 1999).

During the compression and decompression cycles, the pressure in the cavern was designed to fluctuate between a maximum of 5 MPa to a minimum of 2 MPa. The first initial compression took

about 2 days (48 hours) with atmospheric pressure at 5 MPa. Decompression from 5 MPa to 2 MPa was set to take about 19 hours, and the following compression from 2 to 5 MPa took 1.2 days (=24+4.8=28.8 hours). Injection rate was set to 142.6 kg/hour, determined by the specification of the air compressor at the plant, and withdrawal rate was 216.0 kg/hour. These rates respectively correspond to 3.3×10^{-3} kg/s (=142.6 kg/hour / (2 x 6 m x 3600 hour)) and 5.0×10^{-3} kg/s (=216.0 kg/hour / (2 x 6 m x 3600 hour)) for rates applied to the model, with the half-symmetric model domain shown in Figure 9. Simulation results were calculated for 800 hours (approximately 1 month) of multiple compression and withdrawal cycles.

Table 2 presents a set of material properties for the analysis. These properties of deformation modulus and permeability were mainly derived from radial (: Goodman) jacking test and *in situ* site investigations described in the previous section and Poisson's ratio was obtained from the limited number of laboratory tests using drill-core samples from the site. Lee (2012) has reported that porosity in EDZ was increasing to a factor of over 5 after comprehensive laboratory tests of the drilled cores around their underground research tunnel, and considering the embedded fractures *in situ*, we assumed a factor 10 in EDZ porosity. In Table 2, we also include values (within parenthesis) that indicate properties for less compliant EDZ conditions that we used for model comparison. Values for water retention and the relative permeability curve in the van Genuchten model (van Genuchten, 1980) as well as the gas relative permeability governed by Corey's model (Corey, 1954), were referred to previous studies of a tunnel in fractured rock (Finsterle and Pruess, 1995; Alonso et al., 2005). In theory, thermal properties of EDZ could affect the results of thermodynamic analysis especially when wide range of temperature is concerned. However, numerous in situ heater experiments in fractured rock masses such as the Kamaishi mine heater experiment in Japan (Rutqvist et al., 2001), the FEBEX in situ test at Grimsel test site in Switzerland (Alonso et al., 2005) and the Yucca Mountain drift scale test, in Nevada, U.S. (Rutqvist

et al., 2008) have shown a that precise temperature evolution could be predicted by numerical modeling without using different thermal properties in the EDZ. This can be explained by thermal conduction and storage being controlled by matrix thermal properties, whereas fracture porosity is usually very low. Nevertheless, in a CAES system a slight impact of EDZ fractures on thermal properties might have a small impact because heat exchange is confined to within the EDZ, but still the results of this geomechanical analysis would not be significant since the temperature during operation of this underground CAES rarely exceeds 25 $°C$ according to our previous thermodynamic analysis (Kim et al., 2012) so that they were assumed not to change in the analysis.

4.2 Analysis Results

Figure 10 presents the calculated evolution of stress within the concrete lining, and the radial displacement of the inner surface of the concrete lining, under a relatively less compliant EDZ conditions. The minimum principal stress is tensile and increases to a maximum of about 2 MPa (positive stresses signify tensile stress), whereas maximum displacement was less than 0.5 mm. The tensile stress of 2 MPa may result in tensile fracturing of the concrete lining, depending on the strength of the concrete. Figure 11 presents the calculated stress and displacement evolution considering the *in-situ* properties of EDZ and corresponding to more compliant EDZ conditions. We note a minimum principal stress of up to about 4 MPa tensile and a radial displacement of the concrete-lining inner surface exceeding 0.7 mm. This increased tensile stress and radial displacement was caused by an increased compliance of the lining-EDZ-rock system.

The compliance of the EDZ, experienced by the concrete lining is proportional to the elastic Young's modulus. In the less compliant condition, this was 1.0 m / 17.5 GPa = 0.057 m/GPa, whereas in the more compliant condition, it was 0.6 m / 7 GPa = 0.087 GPa/m. Hence, the greater radial displacement was caused by an increment of radial compliance of the system. Moreover,

assuming a softer concrete lining (Young's modulus of 23 GPa compared to 35 GPa for a stiffer case), the total compliance of the EDZ and concrete lining experienced from the inner surface of the lining could be estimated as 0.057 + 0.5 m / 35 GPa = 0.071 m/GPa for the less compliant case and 0.087 + 0.5 m / 23 GPa = 0.109 m/GPa for the more compliant case. This difference implies that the lining system and EDZ in Figure 11 are more compliant by a factor of 0.109 (m/GPa) / 0.071 (m/GPa) = 1.54, directly explaining the increased radial deformation by a factor of 0.72 mm / 0.45mm = 1.5 in the simulation. The increase in tangential stress is related primarily to the increased compliance of the EDZ, since an increased radial displacement, in general, will tend to increase tangential stress.

We carried out more simulations aiming at more precisely investigating the relative effect of the EDZ against the concrete lining. The results are presented in Table 3 in terms of maximum tangential stress and maximum displacement for the first cycle of multiple compression and decompression phases. We note that the maximum radial displacement was small enough to be insignificant from an engineering viewpoint, ranging from 0.46 to 0.73 mm. The magnitude of tangential tensile stress in the concrete lining ranging from 2.4 to 5.26 MPa could be more important for potential tensile fracturing and consequent air leakage through it. It was shown that tensile stress increased with a more compliant EDZ, whereas it decreased with a more compliant concrete lining. Consequently, the highest tangential stress occurred for the case of a relatively compliant EDZ with a stiff concrete lining.

The previous calculations were carried out with a perfectly air tight seal, for example a butyl rubber sheet, at the inner surface of the concrete lining. For the sake of comparison (with the case of C1 in Table 3), we investigated the impact of EDZ compliance on the deformation and stress evolution in the concrete lining without an inner air-tight seal, which may also indicate a partially leaky inner seal. As indicated in Table 3, the permeability of the concrete lining was 7.0×10^{-20} m^2,

while the permeability of the host rock and EDZ was estimated 1.5×10^{-19} and 2.5×10^{-17} m^2, respectively. Kim et al. (2012) showed that a concrete permeability as low as 1.0×10^{-20} m^2 was sufficient to keep air leakage insignificant, regardless of the permeability of the EDZ and surrounding rock mass. We therefore focus our investigation on the tangential stress evolution in the concrete lining, which could potentially lead to fracturing and thus more significant leakage.

Figure 12 presents the evolution of pressure, displacement, and stress for the case of a partially leaky inner seal. Figure 12a shows how pressure within the concrete lining increases with elapsed time. Cavern pressure (P1) fluctuated between the designed pressure range of 2 to 5 MPa, with the pressure in the concrete lining (P2) gradually increasing with time owing to pressurized air penetration through the partially leaky lining. The maximum displacement of the lining and the maximum tangential effective stress peaked at approximately 0.75 mm and 5 MPa, respectively. Thus, the absence of an inner air-tight seal resulted in an increase in tangential stress within the concrete lining from 4 to 5 MPa. Moreover, we observed that the difference between total and effective stresses increased over time as air pressure within the concrete lining increased.

5. Concluding Remarks and Discussions

We investigated the influence of the excavation disturbed zone (EDZ) on the geomechanical performance of compressed air energy storage (CAES) in lined rock caverns. We conducted a detailed characterization of the EDZ in rock caverns that have been constructed for a CAES pilot test program in lined rock caverns at shallow depth. Using the site specific conditions and the results of the *in situ* measurements of EDZ, we then conducted model simulations to investigate the influence of the EDZ on the CAES performance, in particular related to geomechanical responses and stability. We used a modeling approach, coupling thermodynamic, multiphase flow and geomechanics which has been proven useful in previous generic studies of similar CAES systems.

A parameter study showed that the radial displacement and tangential stress in the concrete lining could be effectively reduced if the compliance of the EDZ, defined by EDZ thickness multiplied by EDZ compressibility, could be minimized. It was also noted that a reduction of compliance (increase in stiffness) of the concrete lining resulted in the negligible decrease of radial displacement, but a significant increase of tangential stress that could potentially result in tensile fracturing through the lining. This finding shows that the most favorable design for reducing tensile tangential stress in the lining would be a relatively compliant concrete lining and relatively stiff (uncompliant) rock that is not significantly softened in the EDZ. Because the EDZ compliance depends on its compressibility (or modulus) and thickness, care should be taken during drill-and-blast operations to minimize the damage from the blasting. Finally, our analysis shows the benefit of maintaining an inner impermeable seal that would reduce the effective tensile stress in the concrete and thereby tend to prevent tensile fracturing. Thus, for CAES in lined caverns, we can offer some general recommendations to minimize damage induced by excavation, to reinforce EDZ right after excavation, and to employ an inner impermeable seal. All these actions would help to minimize the risk for pressure induced failure in the concrete lining.

Although the present modeling study could produce a quantitative evaluation of the influence that EDZ compliance has on the geomechanical stability of pressurized lined rock caverns for CAES, further analysis—considering detailed *in situ* conditions, for example the construction joints of inner air-tight seal and concrete linings that would provide predominant pathways for air leakage, should be carried out for large-scale storage caverns. These issues will also be studied *in situ* in upcoming pilot tests.

Acknowledgment

This research was supported by the Basic Research Project of the Korea Institute of Geoscience and Mineral Resources (KIGAM, GP2012-001), funded by the Ministry of Knowledge Economy of Korea, and funding from KIGAM for Dr. Jonny Rutqvist and Berkeley Lab was provided through the U.S. Department of Energy Contract No. DE-AC02-05CH11231. Editorial review by Dan Hawkes at Berkeley Lab is greatly appreciated.

References

Abbas A, Carcasses M, Ollivier JP (1999) Gas permeability of concrete in relation to its degree of saturation. Materials and Structures 32: 3-8

Alonso EE, Alcoverro J, et al., (26 co-authors) (2005) The FEBEX Bechmark test Case definition and comparison of modelling approaches. International Journal of Rock Mechanics and Mining Sciences 42:611-638

Bäckblom G, Martin CD (1999) Recent experiments in hard rocks to study the excavation response: implications for the performance of a nuclear waste geological repository. Tunnelling and Underground Space Technology 14: 377–394

Barton N (2007) Rock quality, seismic velocity, attenuation and anisotropy. Taylor & Francis, Balkema

Bazant P, Kaplan MF (1996) Concrete at high temperature: material properties and mathematical models, Longman

Blümling P, Bernier F, Lebon P, Martin CD (2007) The excavation damaged zone in clay formations time-dependent behaviour and influence on performance assessment. Physics and Chemistry of the Earth 32: 588–599

Bossart P, Peter MM, Moeri A, Trick T, Mayer J (2002) Geological and hydraulic characterization of the excavation disturbed zone in the Opalinus Clay of the Mont Terri Rock Laboratory. Engineering Geology 66: 19–38

Corey AT (1954) The interrelation between oil and gas relative permeabilities. Producers Monthly November: 38-41

Finsterle S, Pruess K (1995) Solving the estimation-identification problem in two-phase flow modeling. Water Resources Research 31: 913-924

Golshani A, Oda M, Okui Y, Takemura T, Munkhtogoo E (2007) Numerical simulation of the excavation damaged zone around an opening in brittle rock. International Journal of Rock Mechanics and Mining Sciences 44(6): 835-845

Hudson JA, Stephansson O, Andersson J, Tsang CF, Jing L (2001) Coupled T-H-M issues relating to radioactive waste repository design and performance, International Journal of Rock Mechanics and Mining Sciences 38(1): 143-161

Itasca. FLAC3D, Fast Lagrangian Analysis of Continua in 3 Dimensions, Version 4.0. Minneapolis, Minnesota, Itasca Consulting Group:2009

Jeong JH. Evaluation of disturbed rock zone using a seismic exploration method. Ph.D. Dissertation. ChonNam National University, Gwangju, Korea:2010

KIGAM (Korea Institute of Geoscience and Mineral Resources). Development of underground energy storage system in lined rock cavern. Seoul, Ministry of Knowledge Economy: 2011

Kim HM, Rutqvist J, Ryu DW, Choi BH, Sunwoo C, Song WK (2012) Exploring the concept of compressed air energy storage (CAES) in lined rock caverns at shallow depth: A modeling study of air tightness and energy balance. Applied Energy 92: 653–667

Kwon S, Cho WJ (2008) The influence of an excavation damaged zone on the thermal-mechanical and hydro-mechanical behaviors of an underground excavation. Engineering Geology 101: 110-123

Lee CS. Characterization of thermal-mechanical behavior of rock mass in the excavation damaged zone at KURT. Ph.D. Dissertation. Seoul National University, Seoul, Korea:2012

Park JM, Kim HC, Lee YM, Song MY (2007) A study on thermal properties of rocks from Gyeonggi-do, Gangwon-do, Chungchung-do, Korea. Economic and Environmental Geology 40(6): 761-769 (in Korean)

Pruess K, Oldenburg C, Moridis G (1999) TOUGH2 User's Guide Version 2.0, LBNL-43134

Rutqvist J. Börgesson L, Chijimatsu M, Nguyen TS, Jing L, Noorishad J, Tsang CF (2001) Coupled thermo-hydro-mechanical analysis of a heater test in fractured rock and bentonite at Kamaishi Mine - Comparison of field results to predictions of four finite element codes. International Journal of Rock Mechanics and Mining Sciences 38: 129–142

Rutqvist J, Freifeld B, Min K-B, Elsworth D, Tsang Y (2008) Analysis of thermally induced changes in fractured rock permeability during eight years of heating and cooling at the Yucca Mountain Drift Scale Test. International Journal Rock Mechanics and Mining Sciences 45: 1373–1389.

Rutqvist J (2011) Status of the TOUGH-FLAC simulator and recent applications related to coupled fluid flow and crustal deformations. Computers and Geosciences 37: 739–750

Rutqvist J, Kim HM, Ryu DW, Synn JH, Song WK (2012) Modeling of coupled thermodynamic and geomechanical performance of underground compressed air energy storage (CAES) in lined rock caverns. International Journal of Rock Mechanics and Mining Sciences 52: 71-81

Sato T, Kikuchi T, Sugihara K (2000) In-situ experiments on an excavation disturbed zone induced by mechanical excavation in Neogene sedimentary rock at Tono mine, central Japan. Engineering Geology 56: 97–108

Succar S, Williams RH (2008) Compressed air energy storage: Theory, resources, and applications for wind power. Princeton Environmental Institute

van Genuchten MT (1980) A closed-form equation for predicting the hydraulic conductivity of unsaturated. Soil Sci Soc Am J 44: 892–898

Wang SH, Lee CI, Ranjith G, Tang CA (2009) Modeling the effects of heterogeneity and anisotropy on the excavation damaged/disturbed zone (EDZ). Rock Mechanics and Rock Engineering 42: 229-258

Table 1. Comparison of average seismic velocities of the EDZ and rock mass

Seismic wave velocity (m/s)	Region	
	EDZ	Rock mass
P wave	1,725	6,430
S wave	950	3,875

Table 2. Material properties used as a base case for modeling of underground CAES in the lined rock cavern

Property	Material		
	Rock mass	Concrete lining	EDZ
Young's modulus, E (GPa)	55.8 (35.0)	23.0 (35.0)	7.0 (35.0)
Poisson's ratio, ν (-)	0.17 (0.3)	0.2 (0.3)	0.25 (0.3)
Thermal expansion coefficient (1/°C)	5.0×10^{-5} [1)] (1.0×10^{-5})	1.2×10^{-5} (1.0×10^{-5})	5.0×10^{-5} (1.0×10^{-5})
Effective porosity, ϕ (-)	0.01	0.01	0.1
Permeability, k, (m^2)	1.5×10^{-19} (1.0×10^{-17})	7×10^{-20} m^2 (1.0×10^{-17})	2.5×10^{-17} (1.0×10^{-20})
Residual gas saturation (-)	0.0	0.0	0.0
Residual liquid saturation (-)	0.01	0.01	0.01
van Genuchten, P_0 (MPa)	1.47	1.47	1.47
Van Genuchten, m (-)	0.595	0.595	0.595
Thermal conductivity λ (J/s/m °K)	3.93 [2)] (3.0)	2.3 [3)] (3.0)	3.93 (3.0)
Specific heat (J/kg °K)	921 [2)] (900)	880 [3)] (900)	921 (900)
Thickness of EDZ (m)	-		0.6 (1.0)

*Numbers within parenthesis indicate the parameters values used in the case of less compliant EDZ for comparison purpose. [1)] JSCE (2006), [2)] Park et al (2007), [3)] Bazant and Kaplan (1996)

Table 3. Effects of different properties of EDZ and concrete on the displacement and stress in the concrete linings of lined rock caverns for underground CAES.

Cases	C1	C2	C3	C4
Young's modulus of EDZ (GPa)	7.0	35.0	7.0	35.0
Young's modulus of concrete lining (GPa)	23.0	23.0	35.0	35.0
Compliance of EDZ $(GPa/mm)^{-1}$	0.086	0.017	0.017	0.086
Compliance of concrete lining $(GPa/mm)^{-1}$	0.022	0.022	0.014	0.014
Total compliance $(GPa/mm)^{-1}$	0.107	0.039	0.031	0.1
Radial displacement at point P4 at the inner surface of concrete lining (mm)	0.73	0.5	0.46	0.66
Tangential effective tensile stress at point P2 in the concrete lining (MPa)	4.07	2.09	2.4	5.26

(Thickness of EDZ and concrete lining were 0.6 m and 0.5 m, respectively)

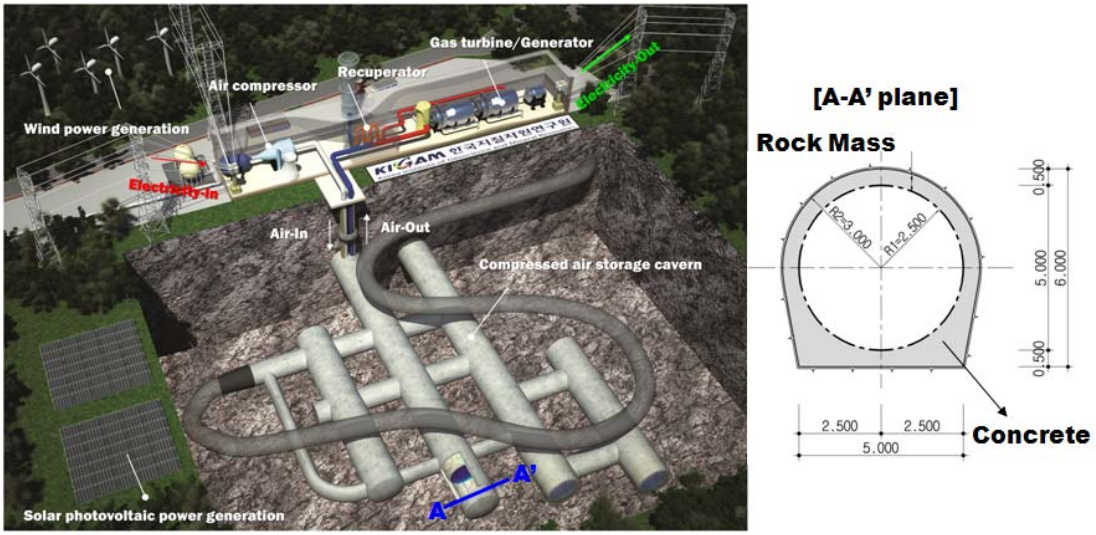

Figure 1. A conceptual diagram of compressed air energy storage (CAES) in lined rock caverns.

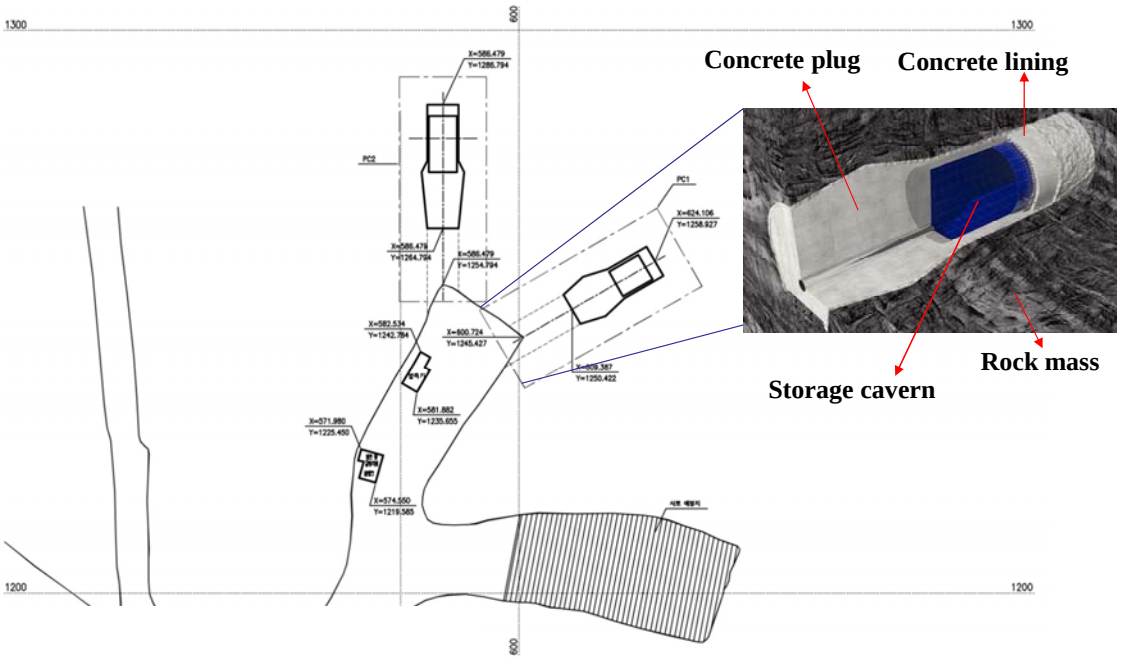

Figure 2. Pilot plant site for underground CAES in limestone at a depth of 100m.

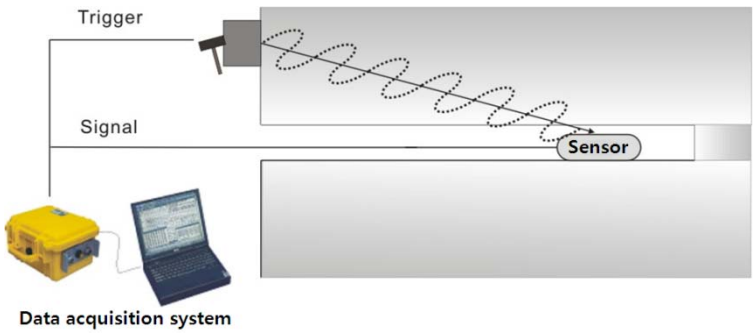

(a)

(b)

(c)

Figure 3. A seismic exploration system for EDZ characterization around excavated cavern: (a) schematic diagram of the system, (b) installation of tri-axial geophone into the borehole, (c) generation of S waves.

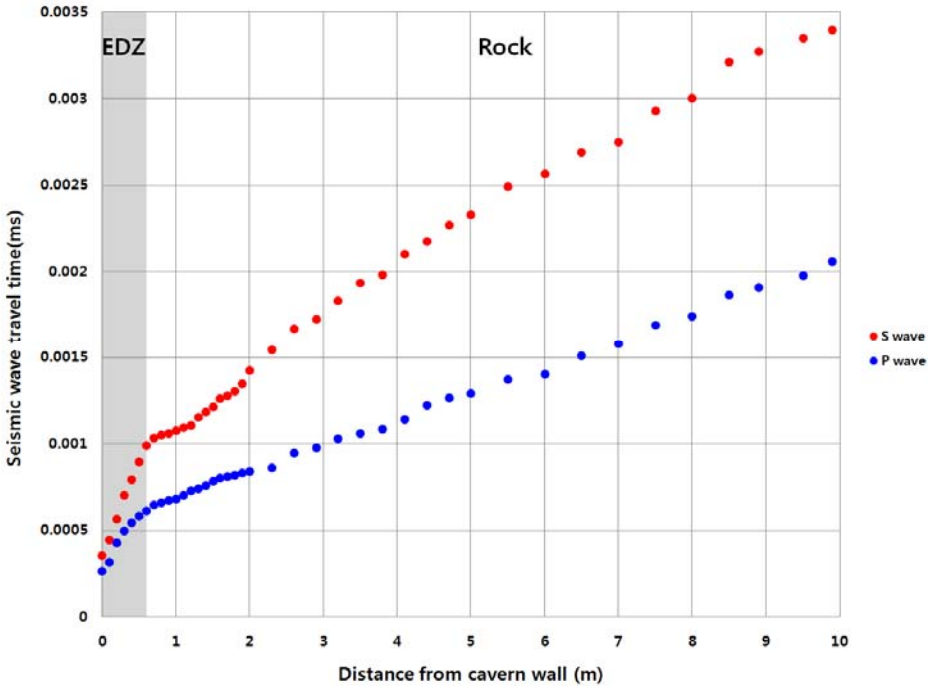

Figure 4. Estimated travel time of seismic wave according to the distance from cavern wall.

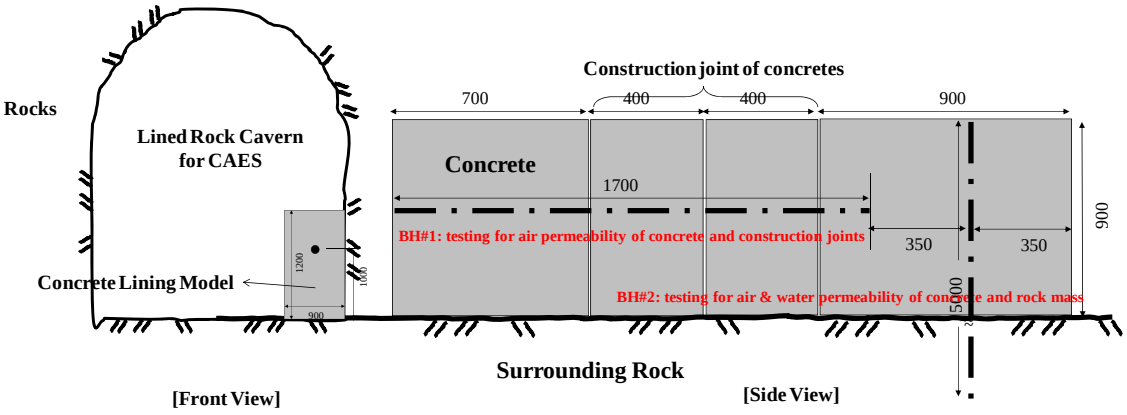

Figure 5. Specification of concrete lining and drilled boreholes for permeability measurement.

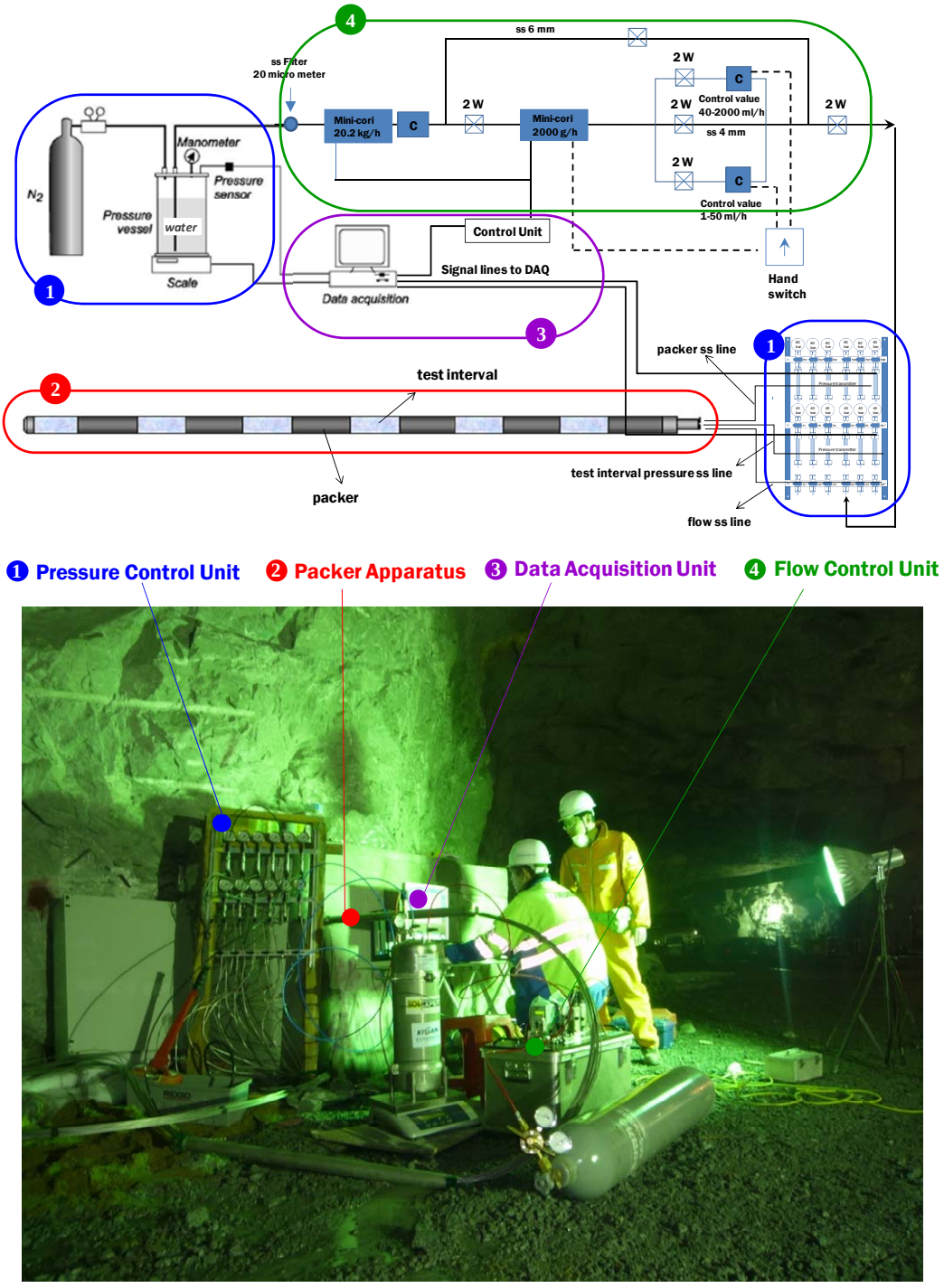

Figure 6. (a) Schematic drawing and (b) installation at the cavern of the pilot plant for CAES of in-situ permeability measurement system for concrete lining and surrounding rock mass.

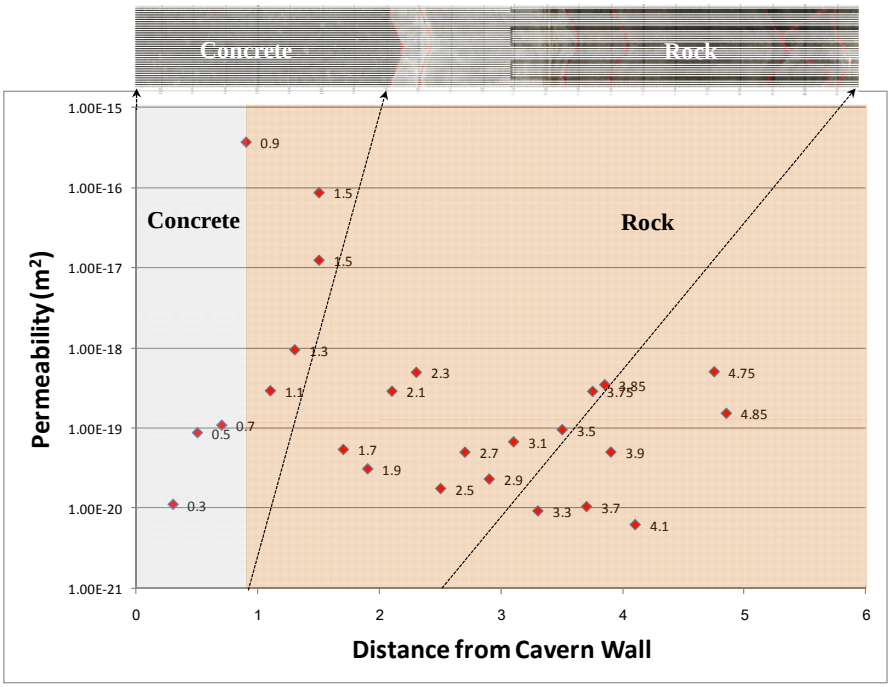

Figure 7. Estimated permeabilities of concrete lining and surrounding rock mass expressed along the distance from excavated rock cavern wall (the red line on the upper borehole wall image shows identified discontinuity and the number on the lower graph indicate the measurement distance from the inner wall of cavern)

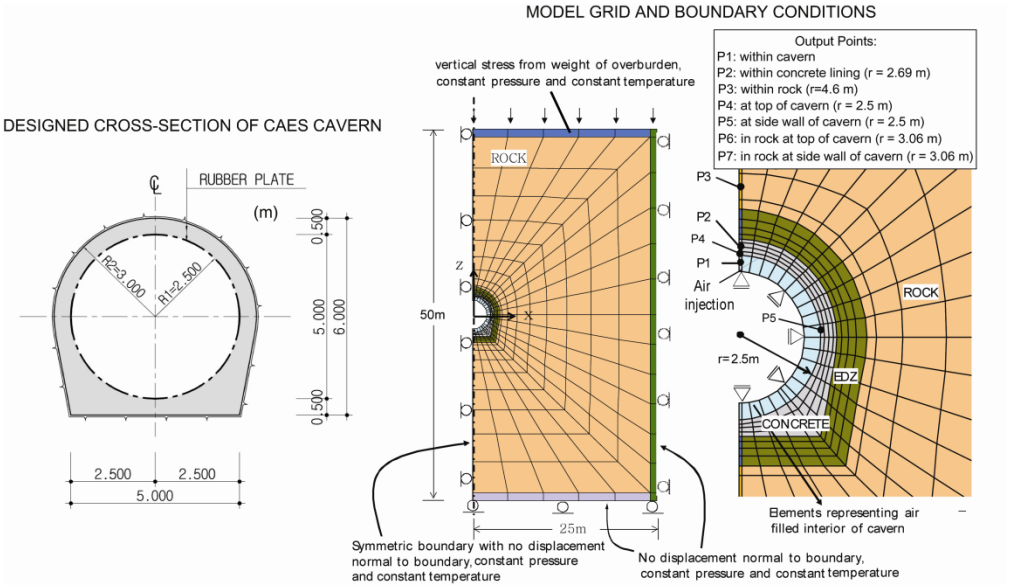

Figure 8. Cross section and model grid used in the analysis (after Kim et al., 2011).

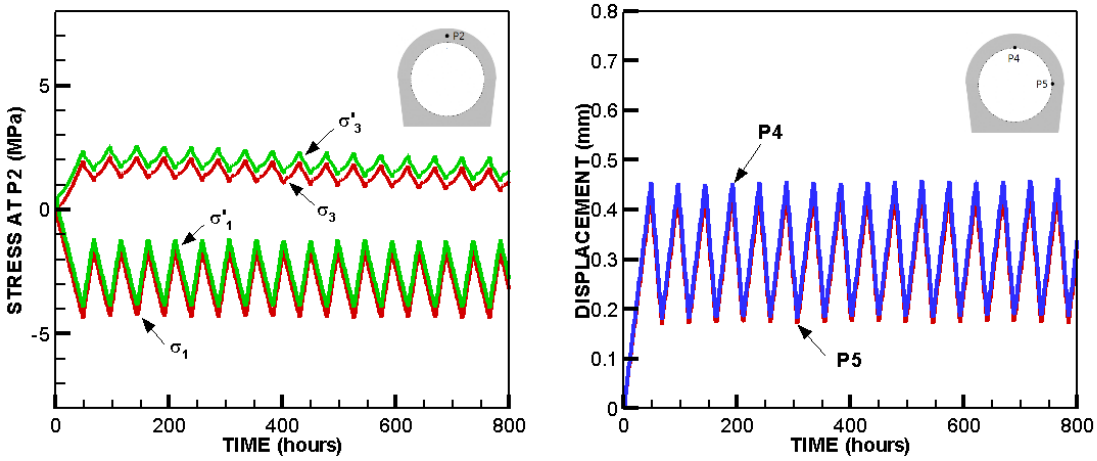

Figure 9. Calculated evolution of (a) stress and (b) displacement of concrete lining in less compliant EDZ condition (See Figure 8 for exact location of P2, P4 and P5).

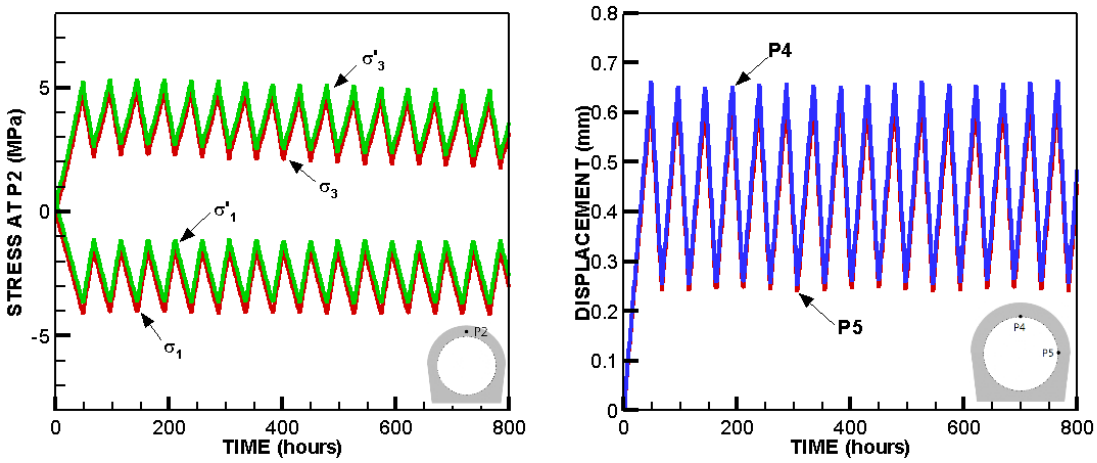

Figure 10. Calculated evolution of (a) stress and (b) displacement of concrete lining in more compliant EDZ condition (See Figure 8 for exact location of P2, P4 and P5).

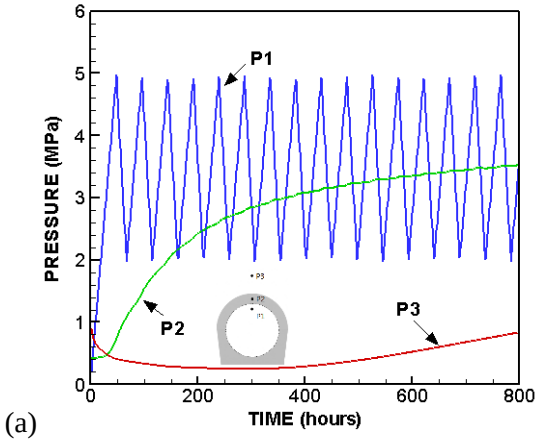

(a)

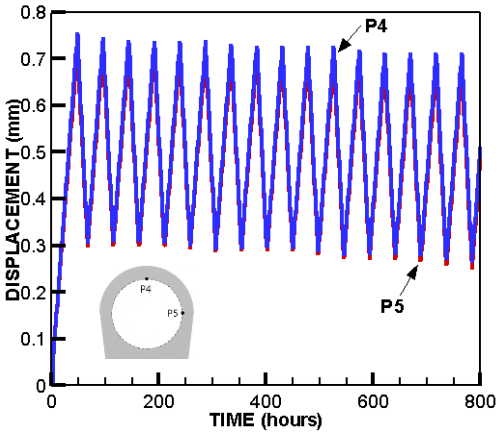

(b)

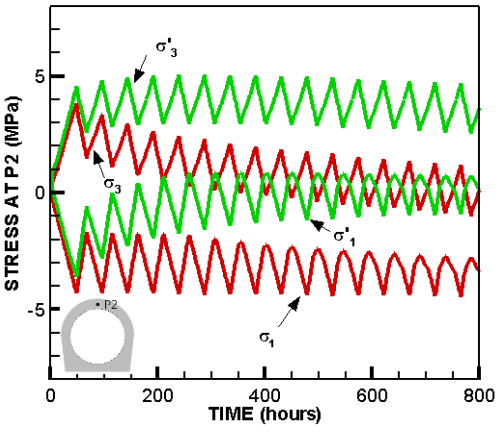

(c)

Figure 11. Calculated evolution of (a) pressure, (b) displacement and (c) stress in consideration of EDZ around concrete lining but without an air tight inner seal inside the concrete lining (See Figure 8 for exact location of P1-P5)..